

First test of Lepton Flavor Universality in the charmed baryon decays $\Omega_c^0 \rightarrow \Omega^- \ell^+ \nu_\ell$ using data of the Belle experiment

Y. B. Li,¹³ C. P. Shen,¹³ I. Adachi,^{19,15} H. Aihara,⁸⁵ S. Al Said,^{79,41} D. M. Asner,³ H. Atmacan,⁸ T. Aushev,²¹ R. Ayad,⁷⁹ V. Babu,⁹ S. Bahinipati,²⁵ P. Behera,²⁸ K. Belous,³² J. Bennett,⁵⁴ F. Bernlochner,² M. Bessner,¹⁸ B. Bhuyan,²⁶ T. Bilka,⁵ A. Bobrov,^{4,64} D. Bodrov,^{21,46} J. Borah,²⁶ A. Bozek,⁶¹ M. Bračko,^{51,38} P. Branchini,³⁴ T. E. Browder,¹⁸ A. Budano,³⁴ M. Campajola,^{33,57} D. Červenkov,⁵ M.-C. Chang,¹² P. Chang,⁶⁰ V. Chekelian,⁵² A. Chen,⁵⁹ B. G. Cheon,¹⁷ K. Chilikin,⁴⁶ H. E. Cho,¹⁷ K. Cho,⁴³ S.-J. Cho,⁹¹ S.-K. Choi,⁷ Y. Choi,⁷⁷ S. Choudhury,³⁶ D. Cinabro,⁸⁹ S. Cunliffe,⁹ N. Dash,²⁸ G. De Nardo,^{33,57} G. De Pietro,³⁴ R. Dhamija,²⁷ F. Di Capua,^{33,57} J. Dingfelder,² Z. Doležal,⁵ T. V. Dong,¹⁰ T. Ferber,⁹ D. Ferlewicz,⁵³ B. G. Fulsom,⁶⁶ R. Garg,⁶⁷ V. Gaur,⁸⁸ N. Gabyshev,^{4,64} A. Giri,²⁷ P. Goldenzweig,³⁹ B. Golob,^{47,38} E. Graziani,³⁴ K. Gudkova,^{4,64} C. Hadjivasiliou,⁶⁶ T. Hara,^{19,15} K. Hayasaka,⁶³ H. Hayashii,⁵⁸ M. T. Hedges,¹⁸ W.-S. Hou,⁶⁰ K. Inami,⁵⁶ G. Inguglia,³¹ A. Ishikawa,^{19,15} R. Itoh,^{19,15} M. Iwasaki,⁶⁵ Y. Iwasaki,¹⁹ W. W. Jacobs,²⁹ E.-J. Jang,¹⁶ S. Jia,¹³ Y. Jin,⁸⁵ K. K. Joo,⁶ J. Kahn,³⁹ K. H. Kang,⁴⁰ T. Kawasaki,⁴² H. Kichimi,¹⁹ C. Kiesling,⁵² C. H. Kim,¹⁷ D. Y. Kim,⁷⁶ K.-H. Kim,⁹¹ K. T. Kim,⁴⁴ Y.-K. Kim,⁹¹ K. Kinoshita,⁸ P. Kodyš,⁵ T. Konno,⁴² A. Korobov,^{4,64} S. Korpar,^{51,38} E. Kovalenko,^{4,64} P. Križan,^{47,38} R. Kroeger,⁵⁴ P. Krokovny,^{4,64} M. Kumar,⁵⁰ R. Kumar,⁶⁹ K. Kumara,⁸⁹ A. Kuzmin,^{4,64,46} Y.-J. Kwon,⁹¹ K. Lalwani,⁵⁰ T. Lam,⁸⁸ M. Laurenza,^{34,72} S. C. Lee,⁴⁵ J. Li,⁴⁵ L. K. Li,⁸ Y. Li,¹³ L. Li Gioi,⁵² J. Libby,²⁸ K. Lieret,⁴⁸ D. Liventsev,^{89,19} A. Martini,⁹ M. Masuda,^{84,70} D. Matvienko,^{4,64,46} S. K. Maurya,²⁶ M. Merola,^{33,57} K. Miyabayashi,⁵⁸ R. Mizuk,^{46,21} G. B. Mohanty,⁸⁰ M. Nakao,^{19,15} D. Narwal,²⁶ A. Natchii,¹⁸ L. Nayak,²⁷ M. Nayak,⁸² N. K. Nisar,³ S. Nishida,^{19,15} K. Ogawa,⁶³ S. Ogawa,⁸³ H. Ono,^{62,63} P. Oskoin,⁴⁶ P. Pakhlov,^{46,55} G. Pakhlova,^{21,46} T. Pang,⁶⁸ S. Pardi,³³ S.-H. Park,¹⁹ S. Patra,²⁴ S. Paul,^{81,52} T. K. Pedlar,⁴⁹ R. Pestotnik,³⁸ L. E. Piilonen,⁸⁸ T. Podobnik,^{47,38} E. Prencipe,²² M. T. Prim,² M. Röhrken,⁹ A. Rostomyan,⁹ N. Rout,²⁸ G. Russo,⁵⁷ D. Sahoo,³⁶ S. Sandilya,²⁷ A. Sangal,⁸ L. Santelj,^{47,38} V. Savinov,⁶⁸ G. Schnell,^{1,23} J. Schueler,¹⁸ C. Schwanda,³¹ Y. Seino,⁶³ K. Senyo,⁹⁰ M. E. Sevier,⁵³ M. Shapkin,³² C. Sharma,⁵⁰ V. Shebalin,¹⁸ J.-G. Shiu,⁶⁰ B. Shwartz,^{4,64} J. B. Singh,^{67,*} A. Sokolov,³² E. Solovieva,⁴⁶ M. Starič,³⁸ Z. S. Stottler,⁸⁸ M. Sumihama,^{14,70} T. Sumiyoshi,⁸⁷ M. Takizawa,^{74,20,71} U. Tamponi,³⁵ K. Tanida,³⁷ F. Tenchini,⁹ M. Uchida,⁸⁶ T. Uglov,^{46,21} Y. Unno,¹⁷ K. Uno,⁶³ S. Uno,^{19,15} P. Urquijo,⁵³ S. E. Vahsen,¹⁸ R. Van Tonder,² G. Varner,¹⁸ A. Vinokurova,^{4,64} E. Waheed,¹⁹ D. Wang,¹¹ E. Wang,⁶⁸ M.-Z. Wang,⁶⁰ S. Watanuki,⁹¹ E. Won,⁴⁴ X. Xu,⁷⁵ B. D. Yabsley,⁷⁸ W. Yan,⁷³ S. B. Yang,⁴⁴ H. Ye,⁹ J. Yelton,¹¹ J. H. Yin,⁴⁴ C. Z. Yuan,³⁰ Y. Yusa,⁶³ Y. Zhai,³⁶ Z. P. Zhang,⁷³ V. Zhilich,^{4,64} and V. Zhukova⁴⁶

(The Belle Collaboration)

¹Department of Physics, University of the Basque Country UPV/EHU, 48080 Bilbao

²University of Bonn, 53115 Bonn

³Brookhaven National Laboratory, Upton, New York 11973

⁴Budker Institute of Nuclear Physics SB RAS, Novosibirsk 630090

⁵Faculty of Mathematics and Physics, Charles University, 121 16 Prague

⁶Chonnam National University, Gwangju 61186

⁷Chung-Ang University, Seoul 06974

⁸University of Cincinnati, Cincinnati, Ohio 45221

⁹Deutsches Elektronen-Synchrotron, 22607 Hamburg

¹⁰Institute of Theoretical and Applied Research (ITAR), Duy Tan University, Hanoi 100000

¹¹University of Florida, Gainesville, Florida 32611

¹²Department of Physics, Fu Jen Catholic University, Taipei 24205

¹³Key Laboratory of Nuclear Physics and Ion-beam Application (MOE)

and Institute of Modern Physics, Fudan University, Shanghai 200443

¹⁴Gifu University, Gifu 501-1193

¹⁵SOKENDAI (The Graduate University for Advanced Studies), Hayama 240-0193

¹⁶Gyeongsang National University, Jinju 52828

¹⁷Department of Physics and Institute of Natural Sciences, Hanyang University, Seoul 04763

¹⁸University of Hawaii, Honolulu, Hawaii 96822

¹⁹High Energy Accelerator Research Organization (KEK), Tsukuba 305-0801

²⁰J-PARC Branch, KEK Theory Center, High Energy Accelerator Research Organization (KEK), Tsukuba 305-0801

²¹National Research University Higher School of Economics, Moscow 101000

²²Forschungszentrum Jülich, 52425 Jülich

- ²³IKERBASQUE, Basque Foundation for Science, 48013 Bilbao
- ²⁴Indian Institute of Science Education and Research Mohali, SAS Nagar, 140306
- ²⁵Indian Institute of Technology Bhubaneswar, Satya Nagar 751007
- ²⁶Indian Institute of Technology Guwahati, Assam 781039
- ²⁷Indian Institute of Technology Hyderabad, Telangana 502285
- ²⁸Indian Institute of Technology Madras, Chennai 600036
- ²⁹Indiana University, Bloomington, Indiana 47408
- ³⁰Institute of High Energy Physics, Chinese Academy of Sciences, Beijing 100049
- ³¹Institute of High Energy Physics, Vienna 1050
- ³²Institute for High Energy Physics, Protvino 142281
- ³³INFN - Sezione di Napoli, I-80126 Napoli
- ³⁴INFN - Sezione di Roma Tre, I-00146 Roma
- ³⁵INFN - Sezione di Torino, I-10125 Torino
- ³⁶Iowa State University, Ames, Iowa 50011
- ³⁷Advanced Science Research Center, Japan Atomic Energy Agency, Naka 319-1195
- ³⁸J. Stefan Institute, 1000 Ljubljana
- ³⁹Institut für Experimentelle Teilchenphysik, Karlsruher Institut für Technologie, 76131 Karlsruhe
- ⁴⁰Kavli Institute for the Physics and Mathematics of the Universe (WPI), University of Tokyo, Kashiwa 277-8583
- ⁴¹Department of Physics, Faculty of Science, King Abdulaziz University, Jeddah 21589
- ⁴²Kitasato University, Sagami-hara 252-0373
- ⁴³Korea Institute of Science and Technology Information, Daejeon 34141
- ⁴⁴Korea University, Seoul 02841
- ⁴⁵Kyungpook National University, Daegu 41566
- ⁴⁶P.N. Lebedev Physical Institute of the Russian Academy of Sciences, Moscow 119991
- ⁴⁷Faculty of Mathematics and Physics, University of Ljubljana, 1000 Ljubljana
- ⁴⁸Ludwig Maximilians University, 80539 Munich
- ⁴⁹Luther College, Decorah, Iowa 52101
- ⁵⁰Malaviya National Institute of Technology Jaipur, Jaipur 302017
- ⁵¹Faculty of Chemistry and Chemical Engineering, University of Maribor, 2000 Maribor
- ⁵²Max-Planck-Institut für Physik, 80805 München
- ⁵³School of Physics, University of Melbourne, Victoria 3010
- ⁵⁴University of Mississippi, University, Mississippi 38677
- ⁵⁵Moscow Physical Engineering Institute, Moscow 115409
- ⁵⁶Graduate School of Science, Nagoya University, Nagoya 464-8602
- ⁵⁷Università di Napoli Federico II, I-80126 Napoli
- ⁵⁸Nara Women's University, Nara 630-8506
- ⁵⁹National Central University, Chung-li 32054
- ⁶⁰Department of Physics, National Taiwan University, Taipei 10617
- ⁶¹H. Niewodniczanski Institute of Nuclear Physics, Krakow 31-342
- ⁶²Nippon Dental University, Niigata 951-8580
- ⁶³Niigata University, Niigata 950-2181
- ⁶⁴Novosibirsk State University, Novosibirsk 630090
- ⁶⁵Osaka City University, Osaka 558-8585
- ⁶⁶Pacific Northwest National Laboratory, Richland, Washington 99352
- ⁶⁷Panjab University, Chandigarh 160014
- ⁶⁸University of Pittsburgh, Pittsburgh, Pennsylvania 15260
- ⁶⁹Punjab Agricultural University, Ludhiana 141004
- ⁷⁰Research Center for Nuclear Physics, Osaka University, Osaka 567-0047
- ⁷¹Meson Science Laboratory, Cluster for Pioneering Research, RIKEN, Saitama 351-0198
- ⁷²Dipartimento di Matematica e Fisica, Università di Roma Tre, I-00146 Roma
- ⁷³Department of Modern Physics and State Key Laboratory of Particle Detection and Electronics, University of Science and Technology of China, Hefei 230026
- ⁷⁴Showa Pharmaceutical University, Tokyo 194-8543
- ⁷⁵Soochow University, Suzhou 215006
- ⁷⁶Soongsil University, Seoul 06978
- ⁷⁷Sungkyunkwan University, Suwon 16419
- ⁷⁸School of Physics, University of Sydney, New South Wales 2006
- ⁷⁹Department of Physics, Faculty of Science, University of Tabuk, Tabuk 71451
- ⁸⁰Tata Institute of Fundamental Research, Mumbai 400005
- ⁸¹Department of Physics, Technische Universität München, 85748 Garching
- ⁸²School of Physics and Astronomy, Tel Aviv University, Tel Aviv 69978
- ⁸³Toho University, Funabashi 274-8510
- ⁸⁴Earthquake Research Institute, University of Tokyo, Tokyo 113-0032
- ⁸⁵Department of Physics, University of Tokyo, Tokyo 113-0033

⁸⁶Tokyo Institute of Technology, Tokyo 152-8550

⁸⁷Tokyo Metropolitan University, Tokyo 192-0397

⁸⁸Virginia Polytechnic Institute and State University, Blacksburg, Virginia 24061

⁸⁹Wayne State University, Detroit, Michigan 48202

⁹⁰Yamagata University, Yamagata 990-8560

⁹¹Yonsei University, Seoul 03722

We present the first observation of the $\Omega_c^0 \rightarrow \Omega^- \mu^+ \nu_\mu$ decay and present measurements of the branching fraction ratios of the $\Omega_c^0 \rightarrow \Omega^- \ell^+ \nu_\ell$ decays compared to the reference mode $\Omega_c^0 \rightarrow \Omega^- \pi^+$, ($\ell = e$ or μ). This analysis is based on 89.5 fb^{-1} , 711 fb^{-1} , and 121.1 fb^{-1} data samples collected with the Belle detector at the KEKB asymmetric-energy e^+e^- collider at the center-of-mass energies of 10.52 GeV, 10.58 GeV, and 10.86 GeV, respectively. The Ω_c^0 signal yields are extracted by fitting $M_{\Omega-\ell^+}$ and $M_{\Omega-\pi^+}$ spectra. The branching fraction ratios $\mathcal{B}(\Omega_c^0 \rightarrow \Omega^- e^+ \nu_e)/\mathcal{B}(\Omega_c^0 \rightarrow \Omega^- \pi^+)$ and $\mathcal{B}(\Omega_c^0 \rightarrow \Omega^- \mu^+ \nu_\mu)/\mathcal{B}(\Omega_c^0 \rightarrow \Omega^- \pi^+)$ are measured to be $1.98 \pm 0.13 \text{ (stat.)} \pm 0.08 \text{ (syst.)}$ and $1.94 \pm 0.18 \text{ (stat.)} \pm 0.10 \text{ (syst.)}$, respectively. The ratio of $\mathcal{B}(\Omega_c^0 \rightarrow \Omega^- e^+ \nu_e)/\mathcal{B}(\Omega_c^0 \rightarrow \Omega^- \mu^+ \nu_\mu)$ is measured to be $1.02 \pm 0.10 \text{ (stat.)} \pm 0.02 \text{ (syst.)}$, which is consistent with the expectation of lepton flavor universality.

In the Standard Model (SM), the charged weak current interaction has an identical coupling to all lepton generations, known as lepton flavor universality (LFU). However, experiments have found tantalizing deviations from LFU in $b \rightarrow c \ell \nu_\ell$ and $b \rightarrow s \ell \ell$ decays [1–6]. The most remarkable result is the recently measured branching fraction ratio $\mathcal{B}(B^+ \rightarrow K^+ \mu^+ \mu^-)/\mathcal{B}(B^+ \rightarrow K^+ e^+ e^-) = 0.846^{+0.044}_{-0.041}$ in the dilepton mass-squared region $1.1 < q^2 < 6.0 \text{ GeV}^2/c^4$ at the LHCb experiment, which is evidence of LFU breaking with a significance of 3.1 standard deviations [7]. Since a violation of LFU is a clear sign of new physics [8–12], tests of LFU in more semileptonic decays of heavy quarks are well motivated.

Lying in the transition region between the perturbative and non-perturbative energy scales of quantum chromodynamics (QCD), charmed baryons play an important role in studies of strong and weak interactions, especially via the investigations of their semileptonic decays [13–15]. Their decay amplitudes are the product of a well-understood leptonic current describing the lepton system and a more complicated hadronic current for the quark transition, which helps to measure SM parameters such as CKM matrix elements and study the details of decay dynamics.

Due to the low production rates and/or high background levels of current experiments, the study of charmed baryon decays is statistically limited. Thus far, semileptonic decays of Λ_c^+ and Ξ_c^0 have only been partially studied, and LFU is found to be conserved within uncertainties [16–19]. The sole result on semileptonic decays of Ω_c^0 is CLEO’s observation of 11.4 ± 3.8 events of $\Omega_c^0 \rightarrow \Omega^- e^+ \nu_e$, with a branching fraction ratio of $\mathcal{B}(\Omega_c^0 \rightarrow \Omega^- e^+ \nu_e)/\mathcal{B}(\Omega_c^0 \rightarrow \Omega^- \pi^+)$ measured to be 2.4 ± 1.2 [20]. Compared with the $\frac{1}{2}^+ \rightarrow \frac{1}{2}^+$ transitions $\Lambda_c^+ \rightarrow \Lambda^0$ and $\Xi_c^0 \rightarrow \Xi^-$, the $\frac{1}{2}^+ \rightarrow \frac{3}{2}^+$ decay $\Omega_c^0 \rightarrow \Omega^-$ contains two more form factors in the hadronic current, which makes it more difficult to predict the decay rate theoretically [21].

The predicted branching fraction $\mathcal{B}(\Omega_c^0 \rightarrow \Omega^- \ell^+ \nu_\ell)$ varies between 0.005 and 0.127 in light-front quark models [21, 22], heavy quark expansion [23], and quark models [24].

We note that the lifetime of Ω_c^0 has been recently updated from $(69 \pm 12) \times 10^{-15} \text{ s}$ [25] to $(268 \pm 26) \times 10^{-15} \text{ s}$ [26, 27]. A precise study of the Ω_c^0 is crucial to test the theoretical models as well as understand the Ω_c^0 lifetime by comparing the measured branching fractions and corresponding theoretical predictions [28–32], especially for its semileptonic decay since constructive interference between the s quarks can result in a large semileptonic decay width [23, 33].

In this Letter, we present a study of the semileptonic decays of $\Omega_c^0 \rightarrow \Omega^- \ell^+ \nu_\ell$ using data samples of 89.5 fb^{-1} , 711 fb^{-1} , and 121.1 fb^{-1} collected by the Belle detector at the KEKB asymmetric-energy collider [34] at the center-of-mass energies of 10.52 GeV, 10.58 GeV, and 10.86 GeV, respectively, which is 66 times larger than the data set used in CLEO’s analysis [20]. Inclusion of charge-conjugate states is implicit unless otherwise stated in this analysis. Ω_c^0 are produced in the process $e^+e^- \rightarrow c\bar{c} \rightarrow \Omega_c^0 + \text{anything}$, while Ω^- baryons are reconstructed via the ΛK^- mode, where Λ decays into $p\pi^-$. Branching fraction ratios of $\Omega_c^0 \rightarrow \Omega^- \ell^+ \nu_\ell$ to the reference mode $\Omega_c^0 \rightarrow \Omega^- \pi^+$ are measured. The precision of $\mathcal{B}(\Omega_c^0 \rightarrow \Omega^- e^+ \nu_e)/\mathcal{B}(\Omega_c^0 \rightarrow \Omega^- \pi^+)$ is significantly improved compared to the previous result [20]. The previously unobserved $\Omega_c^0 \rightarrow \Omega^- \mu^+ \nu_\mu$ decay is also studied. LFU is thus probed in the decays $\Omega_c^0 \rightarrow \Omega^- \ell^+ \nu_\ell$ for the first time.

The Belle detector is a large-solid-angle magnetic spectrometer that consists of a silicon vertex detector, a 50-layer central drift chamber, an array of aerogel threshold Cherenkov counters, a barrel-like arrangement of time-of-flight scintillation counters, and an electromagnetic calorimeter comprised of CsI(Tl) crystals; all these components are located inside a superconducting solenoid coil that provides a 1.5 T

magnetic field. An iron flux-return located outside of the coil is instrumented to detect K_L^0 mesons and identify muons (KLM). The direction of the e^+ momentum is defined as the z -axis direction. The detector is described in detail elsewhere [35].

To optimize the signal selection criteria and calculate the signal reconstruction efficiency, we use Monte Carlo (MC) simulated events. The $e^+e^- \rightarrow c\bar{c}$ process, and the signal Ω_c^0 semileptonic decays are simulated with PYTHIA with matrix element model [36]. The $\Omega_c^0 \rightarrow \Omega^-\pi^+$ decay is generated with EVTGEN [37]. The simulated $\Upsilon(4S) \rightarrow B\bar{B}$, $\Upsilon(5S) \rightarrow B_s^{(*)}\bar{B}_s^{(*)}$, $\Upsilon(5S) \rightarrow B^{(*)}\bar{B}^{(*)}(\pi)$, and $\Upsilon(4S)\gamma$ events with $B = B^+$ or B^0 , and $e^+e^- \rightarrow q\bar{q}$ events with $q = u, d, s$ or c at the center-of-mass energies of data are used as background samples after removing the signal events. The MC events are processed with a detector simulation based on GEANT3 [38]. The background sources and fit methods described later are also validated with simulated generic samples [39].

Except for the charged tracks from Ω^- decays, the impact parameters perpendicular to and along the e^+ beam direction are required to be less than 0.5 cm and 4.0 cm, respectively, and the transverse momentum in the lab frame must be higher than 0.1 GeV/ c . For charged tracks, information from different detector subsystems is combined to form the likelihood \mathcal{L}_i for species i , where $i = e, \mu, \pi, K$, or p [40]. A track with a likelihood ratio $\mathcal{L}_K/(\mathcal{L}_K + \mathcal{L}_\pi) > 0.6$ is identified as a kaon, while a track with $\mathcal{L}_K/(\mathcal{L}_K + \mathcal{L}_\pi) < 0.4$ is treated as a pion [40]. With this selection, the kaon (pion) identification efficiency is about 94% (98%), while 2% (5%) of the pions (kaons) are misidentified as kaons (pions). A track with a likelihood ratio $\mathcal{L}_e/(\mathcal{L}_e + \mathcal{L}_{\text{non-}e}) > 0.9$ is identified as an electron [41]. The γ conversions are suppressed by examining all combinations of an e^\pm track with other oppositely-charged tracks in the event that are identified as e^\mp , and requiring an e^+e^- invariant mass larger than 0.4 GeV/ c^2 . Tracks with $\mathcal{L}_\mu/(\mathcal{L}_\mu + \mathcal{L}_K + \mathcal{L}_\pi) > 0.9$ are considered as muon candidates [42]. The muon tracks are required to hit at least five layers of the KLM subdetector, and not be identified as kaons with $\mathcal{L}_K/(\mathcal{L}_K + \mathcal{L}_\pi) < 0.4$ to suppress backgrounds due to misselection. With the above selections, the efficiencies of electron and muon identifications are 98% and 76%, respectively, with the pion fake rates less than 2%.

The Λ baryons are reconstructed in the decay $\Lambda \rightarrow p\pi^-$ and selected if $|M_{p\pi^-} - m_\Lambda| < 3.5 \text{ MeV}/c^2$ ($\sim 3\sigma$, where σ denotes the mass resolution). Here and throughout the text, M_i represents a measured invariant mass and m_i denotes the nominal mass of the particle i [27]. The proton track from Λ decay is required to satisfy $\mathcal{L}_p/(\mathcal{L}_\pi + \mathcal{L}_p) > 0.2$ and $\mathcal{L}_p/(\mathcal{L}_K + \mathcal{L}_p) > 0.2$ with an efficiency of 95%. Fewer than 1% of the pions/kaons are misidentified as protons/anti-protons. We define the Ω^- signal region as $|M_{\Lambda K^-} - m_{\Omega^-}| < 3.5 \text{ MeV}/c^2$ ($\sim 3\sigma$). Since the background of Ω^- is linear, the Ω^- mass

sidebands are chosen as $13 \text{ MeV}/c^2 < |M_{\Lambda K^-} - m_{\Omega^-}| < 27 \text{ MeV}/c^2$, which is four times the width of the signal region. To suppress the combinatorial background, we require the flight directions of Λ and Ω^- candidates, which are reconstructed from their fitted production and decay vertices, to be within five degrees of their momentum directions in both 3D space and the plane perpendicular to the z -axis in lab frame.

For $\Omega_c^0 \rightarrow \Omega^- e^+ \nu_e$, the cosine of the opening angle between Ω^- and e^+ in the lab frame is further required to be in the region (0.2, 0.95) and the momentum of the e^+ in the center-of-mass frame is required to be in the region (0.35, 1.5) GeV/ c . For $\Omega_c^0 \rightarrow \Omega^- \mu^+ \nu_\mu$, the cosine of the opening angle between Ω^- and μ^+ in the lab frame is required to be larger than 0.35 and the momentum of the μ^+ in the center-of-mass frame should be less than 1.6 GeV/ c .

To suppress combinatorial backgrounds in each of the $\Omega^- e^+ \nu_e$, $\Omega^- \mu^+ \nu_\mu$, and $\Omega^- \pi^+$ modes, we require the scaled momentum $x_p = p_{\Omega^- X}^*/p_{\text{max}}^* > 0.5$, where $p_{\Omega^- X}^*$ is the momentum of the $\Omega^- X$ system in the center-of-mass frame (for $X = e^+, \mu^+$ and π^+ , respectively), and $p_{\text{max}}^* \equiv \sqrt{E_{\text{beam}}^2 - (m_{\Omega_c^0})^2 c^4/c}$ (E_{beam} is the beam energy in the center-of-mass frame). This requirement removes all correct $\Omega^- X$ combinations from Ω_c^0 produced in $B_{(s)}^{(*)}$ decays.

After the above selections, the obtained $M_{\Omega\pi}$, $M_{\Omega e}$, and $M_{\Omega\mu}$ mass spectra from the data samples are shown in Fig. 1. The Ω_c^0 signals are extracted by binned maximum-likelihood fits to these invariant mass spectra. In fitting the $M_{\Omega-\pi^+}$ mass spectrum, the Ω_c^0 signal shape is described by a double-Gaussian function with same mean value, while the background shape is represented with a 1st-order polynomial, where all the parameters are floated. For Ω_c^0 semileptonic decays, the signal shapes are taken directly from MC simulations. The background shapes from wrongly reconstructed Ω^- candidates are described by the $M_{\Omega-\ell^+}$ distributions of Ω^- mass sidebands. The backgrounds from $e^+e^- \rightarrow q\bar{q}$ due to mis-selected ℓ^+ are represented by the $M_{\Omega-\ell^-}$ distributions of $\Omega^- \ell^-$ events with their normalized Ω^- mass sidebands subtracted. The other backgrounds are from $e^+e^- \rightarrow B_{(s)}^{(*)}\bar{B}_{(s)}^{(*)} + \text{anything}$ with Ω^- from one $B_{(s)}^{(*)}$ and ℓ^+ from another $\bar{B}_{(s)}^{(*)}$, whose shapes are taken from simulated data. Background from $\Omega_c^0 \rightarrow \Omega^- \pi^0 \ell^+ \nu_\ell$ decay is negligible since it violates isospin conservation and should be suppressed strongly. In fitting the $\Omega^- \mu^+$ mass spectrum, the $\mu - \pi$ misidentification background component stemming from $\Omega_c^0 \rightarrow \Omega^- \pi^+ + \text{hadrons}$ events is added, with their decay widths set to the PDG values [27]. In the fits to $M_{\Omega-\ell^+}$ spectra above, the shapes of all fit components are fixed, and the yields are floated except for the backgrounds from Ω^- sidebands whose yields are fixed to a quarter of the

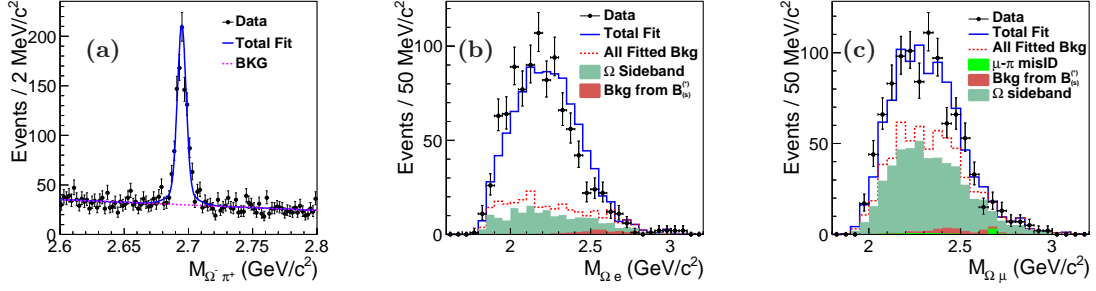


Figure 1: The fits to the (a) $M_{\Omega\pi}$, (b) $M_{\Omega e}$, and (c) $M_{\Omega\mu}$ distributions from the corresponding selected candidates from data. The dots with error bars represent the data, the solid lines are the best fits, and the dashed lines are the fitted total backgrounds. The “ $\mu - \pi$ misID” in plot (c) means the background component from $\Omega_c^0 \rightarrow \Omega^- \pi^+ + \text{hadrons}$ decays. The other fit components are illustrated by the legends.

total number of the sideband events. Figure 1 shows the fitted results for Ω_c^0 decays to (a) $\Omega^- \pi^+$, (b) $\Omega^- e^+ \nu_e$, and (c) $\Omega^- \mu^+ \nu_\mu$. The fitted results together with the corresponding detection efficiencies with the particle identification correction factors included are listed in Table I. The particle identification correction will be described in the systematic part. The significances of the $\Omega_c^0 \rightarrow \Omega^- \ell^+ \nu_\ell$ are both larger than 10σ . The significances are calculated using $\sqrt{-2 \ln(\mathcal{L}_0/\mathcal{L}_{\max})}$, where \mathcal{L}_0 and \mathcal{L}_{\max} are the likelihoods of the fits without and with a signal component, respectively.

Table I: List of the fitted signal yields and the corresponding detection efficiencies with the particle identification correction factors included. The last column gives the ratios of branching fractions $R = \mathcal{B}(\Omega_c^0 \rightarrow \Omega^- \ell^+ \nu_\ell)/\mathcal{B}(\Omega_c^0 \rightarrow \Omega^- \pi^+)$. The branching fractions of $\Omega^- \rightarrow \Lambda K$ and $\Lambda \rightarrow p \pi^-$ are not included in the detection efficiencies. Quoted uncertainties are statistical only.

channel	signal yields	detection efficiency	R
$\Omega_c^0 \rightarrow \Omega^- \pi^+$	865.3 ± 35.3	18.87%	...
$\Omega_c^0 \rightarrow \Omega^- e^+ \nu_e$	707.6 ± 37.7	7.40%	1.98 ± 0.13
$\Omega_c^0 \rightarrow \Omega^- \mu^+ \nu_\mu$	367.9 ± 31.4	3.93%	1.94 ± 0.18

The Ω_c^0 semileptonic decay branching fraction ratios are calculated using

$$\frac{\mathcal{B}(\Omega_c^0 \rightarrow \Omega^- \ell^+ \nu_\ell)}{\mathcal{B}(\Omega_c^0 \rightarrow \Omega^- \pi^+)} = \frac{N_{\Omega\ell} \cdot \varepsilon_{\Omega\pi}}{N_{\Omega\pi} \cdot \varepsilon_{\Omega\ell}},$$

where N and ε are the fitted signal yields and detector efficiency of the corresponding Ω_c^0 decay, respectively. The calculated results are listed in Table I. Similarly, we also obtain $\mathcal{B}(\Omega_c^0 \rightarrow \Omega^- e^+ \nu_e)/\mathcal{B}(\Omega_c^0 \rightarrow \Omega^- \mu^+ \nu_\mu) = 1.02 \pm 0.10$. Here, the uncertainties are statistical only.

Several sources of systematic uncertainties contribute to the measurement of the branching fraction ratios. Using $D^{*+} \rightarrow D^0 \pi^+$, $D^0 \rightarrow K^- \pi^+$, and $J/\psi \rightarrow \ell\ell$ control samples, the efficiency ratios between data

and MC simulations are $(95.4 \pm 0.9)\%$, $(98.2 \pm 0.9)\%$, and $(98.7 \pm 0.6)\%$ for pion, electron, and muon, respectively. The central values of the ratios are taken as the efficiency correction factors and the errors are taken as systematic uncertainties, written as σ_{PID} . The systematic uncertainties associated with tracking efficiency and Ω^- selection approximately cancel in the branching fraction ratio measurements so that the uncertainties on those are negligible. We estimate the systematic uncertainties associated with the fitting procedures (σ_{fit}) for $\Omega_c^0 \rightarrow \Omega^- \ell^+ \nu_\ell$ and $\Omega_c^0 \rightarrow \Omega^- \pi^+$ separately. For $\Omega_c^0 \rightarrow \Omega^- \ell^+ \nu_\ell$ decays, we change the bin width of the $M_{\Omega-\ell^+}$ spectra by $\pm 5 \text{ MeV}/c^2$, change the Ω^- mass sidebands from four to three times that of the signal region, and take the differences of the fitted signal yields as σ_{fit} : these are 1.0% for the electron mode and muon mode. For $\Omega_c^0 \rightarrow \Omega^- \pi^+$, we estimate σ_{fit} by changing the range of the fit and the order of the background polynomial, and take the difference of the signal yields, 0.4%, as the systematic uncertainty. For $\Omega_c^0 \rightarrow \Omega^- \pi^+$, the x_p distribution is corrected with efficiencies bin by bin, and is fitted with Peterson’s fragmentation function $1/(x_p \cdot (1 - \frac{1}{x_p} - \frac{\epsilon_p}{1-x_p})^2)$ [43]. The signal MC samples of all three decay modes are generated with the fitted Peterson’s fragmentation function, and the difference of the detection efficiencies obtained by changing the fitted ϵ_p by $\pm 1\sigma$ are taken as the systematic uncertainty (σ_{x_p}), which are 0.5%, 0.5%, and 2.1% for electron, muon, and pion mode, respectively. For semileptonic decays, to conservatively estimate the uncertainties due to possible imperfect modeling by PYTHIA matrix element model, the signal MC samples of $\Omega_c^0 \rightarrow \Omega^- \ell^+ \nu_\ell$ decays are simulated with phase space model. The changes in measured branching fractions are taken as the uncertainties of MC model (σ_{MC}).

The changes of the measured branching fractions by fitting the $M_{\Omega\ell}$ spectra without the background

component from $B_{(s)}^{(*)}$ decays are taken as the uncertainties due to $B_{(s)}^{(*)}$ decay ($\sigma_{B_{(s)}^{(*)}}$), which are 2.6% and 3.0% for the electron and muon mode, respectively. The relative systematic uncertainties above are summarized in Table II.

Table II: The relative systematic uncertainties on the branching fraction measurements (%).

channel	σ_{PID}	σ_{fit}	σ_{x_p}	σ_{MC}	$\sigma_{B_{(s)}^{(*)}}$	total
$\Omega_c^0 \rightarrow \Omega^- \pi^+$	0.9	0.4	2.1	2.3
$\Omega_c^0 \rightarrow \Omega^- e^+ \nu_e$	0.9	1.0	0.5	2.6	1.4	3.3
$\Omega_c^0 \rightarrow \Omega^- \mu^+ \nu_\mu$	0.6	1.0	0.5	3.0	2.8	4.3

The corresponding systematic uncertainties above are summed in quadrature to yield the total systematic uncertainty (σ_B) for each Ω_c^0 decay mode, which yields 2.3%, 3.3%, and 4.3% for the pion, electron, and muon mode, respectively. The final systematic uncertainty of the branching fraction ratio is the sum of the corresponding two σ_B in quadrature, which yields 4.0% and 4.9% for $\mathcal{B}(\Omega_c^0 \rightarrow \Omega^- \ell^+ \nu_\ell)/\mathcal{B}(\Omega_c^0 \rightarrow \Omega^- \pi^+)$, with $\ell^+ = e^+$ and μ^+ , respectively. The total systematic uncertainty on $\mathcal{B}(\Omega_c^0 \rightarrow \Omega^- e^+ \nu_e)/\mathcal{B}(\Omega_c^0 \rightarrow \Omega^- \mu^+ \nu_\mu)$ is 2.3% with the $\sigma_{B_{(s)}^{(*)}}$, σ_{x_p} , and σ_{MC} positively correlated.

According to the analysis above, the branching fraction ratios $\mathcal{B}(\Omega_c^0 \rightarrow \Omega^- e^+ \nu_e)/\mathcal{B}(\Omega_c^0 \rightarrow \Omega^- \pi^+)$ and $\mathcal{B}(\Omega_c^0 \rightarrow \Omega^- \mu^+ \nu_\mu)/\mathcal{B}(\Omega_c^0 \rightarrow \Omega^- \pi^+)$ are measured to be $1.98 \pm 0.13 \pm 0.08$ and $1.94 \pm 0.18 \pm 0.10$, respectively. The ratio $\mathcal{B}(\Omega_c^0 \rightarrow \Omega^- e^+ \nu_e)/\mathcal{B}(\Omega_c^0 \rightarrow \Omega^- \pi^+)$ is consistent with the previously measured value 2.4 ± 1.2 by the CLEO collaboration [20] with greatly improved precision. The ratio of $\mathcal{B}(\Omega_c^0 \rightarrow \Omega^- e^+ \nu_e)/\mathcal{B}(\Omega_c^0 \rightarrow \Omega^- \mu^+ \nu_\mu)$ is measured to be $1.02 \pm 0.10 \pm 0.02$, which is consistent with the expectation of LFU [22]. Here, the first and second uncertainties are statistical and systematic, respectively.

In summary, based on data samples of 89.5, 711 and 121.1 fb $^{-1}$ collected with the Belle detector at the center-of-mass energies of 10.52, 10.58, and 10.86 GeV, respectively, we measured the branching fraction ratios of $\mathcal{B}(\Omega_c^0 \rightarrow \Omega^- \ell^+ \nu_\ell)/\mathcal{B}(\Omega_c^0 \rightarrow \Omega^- \pi^+)$ and $\mathcal{B}(\Omega_c^0 \rightarrow \Omega^- e^+ \nu_e)/\mathcal{B}(\Omega_c^0 \rightarrow \Omega^- \mu^+ \nu_\mu)$. The $\Omega_c^0 \rightarrow \Omega^- \mu^+ \nu_\mu$ decay is seen for the first time. Our measured $\mathcal{B}(\Omega_c^0 \rightarrow \Omega^- \ell^+ \nu_\ell)/\mathcal{B}(\Omega_c^0 \rightarrow \Omega^- \pi^+)$ are larger than those from the predictions of the light-front quark models [21, 22], and $\mathcal{B}(\Omega_c^0 \rightarrow \Omega^- e^+ \nu_e)/\mathcal{B}(\Omega_c^0 \rightarrow \Omega^- \mu^+ \nu_\mu)$ agrees with the expectation of LFU. The values of $\mathcal{B}(\Omega_c^0 \rightarrow \Omega^- \ell^+ \nu_\ell)$ will be able to be derived and compared with theoretical expectations and those of other semileptonic decays of charmed baryons once the value of $\mathcal{B}(\Omega_c^0 \rightarrow \Omega^- \pi^+)$ has been measured.

Y. B. Li acknowledges the support from China Postdoctoral Science Foundation (2020TQ0079). We thank the KEKB group for excellent operation of the

accelerator; the KEK cryogenics group for efficient solenoid operations; and the KEK computer group, the NII, and PNNL/EMSL for valuable computing and SINET5 network support. We acknowledge support from MEXT, JSPS and Nagoya's TLPSC (Japan); ARC (Australia); FWF (Austria); the National Natural Science Foundation of China under Contracts No. 11575017, No. 11761141009, No. 11975076, No. 12042509, No. 12135005, No. 12161141008; MSMT (Czechia); ERC Advanced Grant 884719 and Starting Grant 947006 (European Union); CZF, DFG, EXC153, and VS (Germany); DAE (Project Identification No. RTI 4002) and DST (India); INFN (Italy); MOE, MSIP, NRF, RSRI, FLRFAS project, GSDC of KISTI and KREONET/GLORIAD (Korea); MNiSW and NCN (Poland); MSHE, Agreement No. 14.W03.31.0026, and HSE UBRC (Russia); University of Tabuk (Saudi Arabia); ARRS Grants J1-9124 and P1-0135 (Slovenia); IKERBASQUE (Spain); SNSF (Switzerland); MOE and MOST (Taiwan); and DOE and NSF (USA).

* also at University of Petroleum and Energy Studies, Dehradun 248007

- [1] Y. S. Amhis *et al.* (HFLAV Collaboration), *Eur. Phys. J. C* **81** 226 (2021).
- [2] R. Aaij *et al.* (LHCb Collaboration), *Phys. Rev. Lett.* **122**, 191801 (2019).
- [3] R. Aaij *et al.* (LHCb Collaboration), *JHEP* **08**, 055 (2017).
- [4] J.P. Lees *et al.* (BaBar Collaboration), *Phys. Rev. Lett.* **109**, 101802 (2012).
- [5] R. Aaij *et al.* (LHCb Collaboration), *Phys. Rev. Lett.* **120**, 171802 (2018).
- [6] R. Aaij *et al.* (LHCb Collaboration), *Phys. Rev. D* **94**, 072007 (2016).
- [7] R. Aaij *et al.* (LHCb Collaboration), *arXiv:2103.11769*.
- [8] D. Bećirević, S. Fajfer, N. Košnik, and O. Sumensari, *Phys. Rev. D* **94**, 115021 (2016).
- [9] A. Crivellin, D. Müller, and T. Ota, *JHEP* **09**, 040 (2017).
- [10] D. Buttazzo, A. Greljo, G. Isidori, and D. Marzocca, *JHEP* **11**, 044 (2017).
- [11] W. Altmannshofer, S. Gori, S. Profumo, and F. S. Queiroz, *JHEP* **12**, 106 (2016).
- [12] A. J. Buras and J. Girrbach, *JHEP* **12**, 009 (2013).
- [13] J. D. Richman and P. R. Burchat, *Rev. Mod. Phys.* **67**, 893 (1995).
- [14] E. Eichten and B. Hill, *Phys. Lett. B* **234**, 511 (1990).
- [15] M. Neubert, *Phys. Rep.* **245**, 259 (1994).
- [16] M. Ablikim *et al.* (BESIII Collaboration), *Phys. Rev. Lett.* **115**, 221805 (2015).
- [17] M. Ablikim *et al.* (BESIII Collaboration), *Phys. Lett. B* **767**, 42 (2017).
- [18] M. Ablikim *et al.* (BESIII Collaboration), *Phys. Rev. Lett.* **121**, 251801 (2018).
- [19] Y. B. Li *et al.* (Belle Collaboration), *Phys. Rev. Lett.* **127**, 121803 (2021).
- [20] R. Ammar *et al.* (CLEO Collaboration), *Phys. Rev. Lett.*

- 89**, 171803 (2002).
- [21] Y. K. Hsiao, L. Yang, C. C. Lih, and S. Y. Tsai, *Eur. Phys. J. C* **80**, 1066 (2020).
 - [22] F. Huang and Q. A. Zhang, [arXiv:2108.06110 \(2021\)](#).
 - [23] M. B. Voloshin, *Phys. Lett. B* **385**, 369 (1996).
 - [24] M. Pervin, W. Roberts, and S. Capstick, *Phys. Rev. C* **74**, 025205 (2006).
 - [25] M. Tanabashi et al. (Particle Data Group), *Phys. Rev. D* **98**, 030001 (2018).
 - [26] R. Aaij et al. (LHCb Collaboration), *Phys. Rev. Lett.* **121**, 092003 (2018).
 - [27] P. A. Zyla et al. (Particle Data Group), *Prog. Theor. Exp. Phys.* **2020**, 083C01 (2020).
 - [28] S. Bianco, F. L. Fabbri, D. Benson, and I. Bigi, *Riv. Nuovo Cim.* **26**, 1 (2003).
 - [29] H. Y. Cheng, *Phys. Rev. D* **56**, 2783 (1997).
 - [30] G. Bellini, I. I. Y. Bigi, and P. J. Dornan, *Phys. Rept.* **289**, 1 (1997).
 - [31] B. Blok and M. Shifman, [arXiv:hep-ph/9311331 \(1993\)](#).
 - [32] H. Y. Cheng, [arXiv:2109.01216 \(1997\)](#).
 - [33] B. Guberina and B. Melic, *Eur. Phys. J. C* **2**, 697-703 (1998).
 - [34] S. Kurokawa and E. Kikutani, *Nucl. Instrum. Methods Phys. Res., Sect. A* **499**, 1 (2003), and other papers included in this volume; T. Abe et al., *Prog. Theor. Exp. Phys.* **2013**, 03A001 (2013) and following articles up to 03A011.
 - [35] A. Abashian et al. (Belle Collaboration), *Nucl. Instrum. Methods Phys. Res., Sect. A* **479**, 117 (2002); also, see detector section in J. Brodzicka et al., *Prog. Theor. Exp. Phys.* **2012**, 04D001 (2012).
 - [36] T. Sjöstrand et al., *Comput. Phys. Commun.* **135**, 238 (2001).
 - [37] D. J. Lange, *Nucl. Instrum. Methods Phys. Res., Sect. A* **462**, 152 (2001).
 - [38] R. Brun et al., GEANT, CERN Report No. DD/EE/84-01 (1984).
 - [39] X. Zhou, S. Du, G. Li, and C. Shen, *Comput. Phys. Commun.* **258**, 107540 (2021).
 - [40] E. Nakano, *Nucl. Instrum. Methods Phys. Res., Sect. A* **494**, 402 (2002).
 - [41] K. Hanagaki et al., *Nucl. Instrum. Methods Phys. Res., Sect. A* **485**, 490 (2002).
 - [42] A. Abashian et al., *Nucl. Instrum. Methods Phys. Res., Sect. A* **491**, 69 (2002).
 - [43] C. Peterson et al., *Phys. Rev. D* **27**, 105 (1983).